

Fermi-Polaron in a driven-dissipative background medium

Ye Cao^{1,*} and Jing Zhou^{2,†}

¹*School of Physics, Beijing Institute of Technology, Beijing 100081, China*

²*Department of Science, Chongqing University of Posts and Telecommunications, Chongqing 40006, China*

(Dated: June 22, 2022)

The study of polaron of an open quantum system plays an important role in both verifying the effectiveness of approximate many-body theory and predicting novel quantum phenomenon in open quantum systems. In a pioneering work, Piazza et al have proposed a Fermi-polaron scheme with a lossy impurity [54], which exhibits a novel long-lived attractive polaron branch in the quantum Zeno limit. However, we would also run into a counterpart problem that an impurity scatters with an open quantum bath exciting polarons, which is what we focus in on. In this work, we conclude the molecular state under the two limits of vanishing small and infinite large dissipation intensity as well as the reason why the dissipation range leads to the decrease of the gap between the molecular state and molecule-hole continuum in the former case by means of analytically research. The spectrum functions of molecular and polaron states with different dissipation range and loss rate are investigated. We find the spectral signals of molecular and polaron states will both diffuse firstly and then revives as the dissipation is on the raise. Moreover, it is shown that the attractive and repulsive polarons show different response to the increasing dissipation range in our model. At last, we exhibit the polaron energy, residue, effective mass and two-body decay for mass balanced and imbalanced systems. Our results might be useful for future cold atom experiment on open quantum systems.

I. INTRODUCTION

Since the concept of polaron was proposed as quasiparticles arising from the electron-phonon interaction in the 1930s [1], the mechanism of a mobile impurity interacting with its environment has gained widespread concern. It plays a key role in understanding the low-energy behavior of complex systems, e.g., cuprate superconductors [2], colossal magnetoresistive manganites [3], ³He-⁴He mixtures [4], and promising organic semiconductors [5], to name a few.

Due to the excellent flexibility, the ultracold atomic system has attracted extensive attention in recent years [6, 7]. Especially, the progress of the study on polaron continues to spring up in our times, both experimentally [8–18] and theoretically [19–45]. However, these investigations are restricted to isolated systems. With the development of quantum physics, the open quantum systems have become more and more significant. The non-negligible coupling of some specific systems with their environments, the diseconomy and difficulty of calculating a large isolated system and removing overwhelming useless information to obtain the specific degree of freedom which we pay attention to, are a couple of reasons why the theory of open quantum system plays such a crucial role.

Further more, dissipation has been proved to be pivotal in the production of novel quantum phenomenas. Many breakthroughs have been made in the theoretical and experimental areas. For instance, dissipation can in-

duce strong correlation in ultracold Bosonic atoms [46] and controll phase transition from the Mott insulator to the superfluid [47], slow down the relaxation of many-body states to an algebraic law [48], engineer tunable local loss in a synthetic lattice of momentum state [49], and bring about \mathcal{PT} -symmetry-breaking transitions that makes a \mathcal{PT} -symmetric broken phase which is beyond the quantum Zeno effect comes into being [50]. From another perspective, as an effective theory to describe the system undergoing dissipation, the non-Hermitian Hamiltonian approach has aroused great interest in recent years [51], inspiring the research from the aspects of skin effect, dynamics, band theory, topological phase-transition, non-Hermitian linear response theory, non-Hermitian semimetal and dissipation-facilitated molecule and so on.

Nevertheless, to the best of our knowledge, the works about dissipative polaron [52–54] are still rare. On the one hand, benefiting from the simplicity, polaron physics is suitable for checking the consistency of many-body theory and experimental results. As a pioneering work [54], Piazza et. al. have considered a polaron scheme that the impurity atom bears driving and dissipation which do not come from the bath but from other environment degrees, where they found quantum Zeno effect in the impurity spectrum function. On the other hand, another important mission of a polaron is to act as a probe of its bath, e.g., a complex open quantum system which we make concern of. Based on the importance of many-body theory for a quantum open system and the thirst for knowledge of open quantum system which is difficult to calculate, it is worthwhile to carry out new polaron studies, in the scenario of which the bath is dissipated and driven by its own environment.

In this work, we study a new polaron system whereby

* These authors contributed equally to this work.

† These authors contributed equally to this work.; corresponding author: zhjing@mail.ustc.edu.cn

the bath turns to be Fermi gases suffering external driving and dissipation. In order to take the effect of quantum jump term of the Lindblad master equation (LMEQ) into account, we commence the study with the total action function of the impurity and background gases. Employing the non-equilibrium Green's function (GF) method, we present the spectrum responses of molecular and polaron states under different system configurations. We also calculate quasiparticle parameters in both mass balanced and imbalanced polaron setup, which can be realized in the experiments. Two analytic results are obtained. Firstly, for the vanishingly small dissipation, we explain the reason why the gap between molecular state and molecule-hole continuum decreases with the increase of dissipation range. Secondly, for the infinite dissipation, we obtain the dispersion of bound state as well as the threshold of molecule-hole continuum. We find the resonant peaks of molecular and polaron states become diffuse only under moderate dissipation. On the contrary, they become well-defined with infinite dissipation. In other words, under this limit, the dissipation range only plays a role in reconstructing the Fermi surface. This mechanism is consistent with the Zeno effect described in [54, 59]. The residue, effective mass and two-body decay show nonmonotonic characters due to the interplay between the intrinsic energy scale of the system and the measurement frequency from the environment. However, they all tend to respective saturation values under the Zeno limit.

The paper is organized as follows: in Sec. II, we introduce our model and Keldysh diagrammatic approach to our dissipative polaron problem. In Sec. III, we discuss the numerical results of the molecular and the polaron states. In Sec. IV, we make a conclusion and give some remarks and outlook on this research topic.

II. MODEL AND ANALYTICAL APPROACH

A. Model Hamiltonian and LMEQ

Let us consider a system composed of a fermionic impurity and a two-dimensional open Fermi bath interacting with it. The Hamiltonian is expressed as

$$\mathcal{H} = \mathcal{H}_{\text{imp}} + \mathcal{H}_{\text{bath}} + \mathcal{H}_{\text{int}}, \quad (1)$$

where $\mathcal{H}_{\text{imp}} = \sum_{\mathbf{k}} \varepsilon_c(\mathbf{k}) c_{\mathbf{k}}^\dagger c_{\mathbf{k}}$ and $\mathcal{H}_{\text{bath}} = \sum_{\mathbf{k}} \varepsilon_f(\mathbf{k}) f_{\mathbf{k}}^\dagger f_{\mathbf{k}}$ are the kinetic Hamiltonians of impurity and bath, the dispersions of which are $\varepsilon_c(\mathbf{k}) = \mathbf{k}^2/2m_c$ and $\varepsilon_f(\mathbf{k}) = \mathbf{k}^2/2m_f$, respectively. $\mathcal{H}_{\text{int}} = g \int d\mathbf{r} c^\dagger(\mathbf{r}) c(\mathbf{r}) f^\dagger(\mathbf{r}) f(\mathbf{r})$ is the s -wave contact interaction between the impurity and the bath. The dynamics of the bath should be describe by a LMEQ,

$$\partial_t \rho_{\text{bath}} = -i[\mathcal{H}_{\text{bath}}, \rho_{\text{bath}}(t)] + \mathcal{L}_d \rho_{\text{bath}}(t), \quad (2)$$

where the \mathcal{L}_d is the dissipative Lindblad operator, whose effect on the density operator is $\mathcal{L}_d \rho_{\text{bath}} =$

$\sum_{\mathbf{k}} \{\gamma(\mathbf{k}) D[f_{\mathbf{k}}] + \Omega(\mathbf{k}) P[f_{\mathbf{k}}]\} \rho_{\text{bath}}$, describing loss and reinjection of particles with rate of $\gamma(\mathbf{k})$ and $\Omega(\mathbf{k})$. The two incoherent processes are induced by the superoperators, $D[f_{\mathbf{k}}] \rho_{\text{bath}} \equiv f_{\mathbf{k}} \rho_{\text{bath}} f_{\mathbf{k}}^\dagger - \frac{1}{2} \{f_{\mathbf{k}}^\dagger f_{\mathbf{k}}, \rho_{\text{bath}}\}$ and $P[f_{\mathbf{k}}] \equiv -D[f_{\mathbf{k}}] + D[f_{\mathbf{k}}^\dagger]$, where we have chosen a specific pumping behavior for simplicity. The action of $D[f_{\mathbf{k}}]$ operating on the density matrix ρ_{bath} results in two processes, one is the continuous nonunitary evolution coming from the anticommutator term, the other one is quantum jump produced by $f_{\mathbf{k}} \rho_{\text{bath}} f_{\mathbf{k}}^\dagger$. The former describes the continuous losses of energy and information in the process of decoherence with environment, and the later represents the continuous measurement of the system.

For our model, there is not interaction between the bath atoms, so the matrix representing of the density operator is block diagonal in bases of the Fock states for each momentum. Further more, the bath is supposed to keep in a steady state where the loss and pump are already in equilibrium, therefore the matrix elements of the density matrix is time independent that can be find out through the LMEQ as $\rho_{\mathbf{k}}^{00} = 1 - \Omega(\mathbf{k})/\gamma(\mathbf{k})$, $\rho_{\mathbf{k}}^{01} = 0$, $\rho_{\mathbf{k}}^{11} = \Omega(\mathbf{k})/\gamma(\mathbf{k})$. In addition, the underlying probability annotation of the density operator requires that the ratio $\Omega(\mathbf{k})/\gamma(\mathbf{k})$ must be confined in the range of $[0, 1]$. For each momentum, the average particle number is determined by this ratio, the momentum distribution of which further establishes the average total particle number.

B. T -matrix method with Non-equilibrium Green's function

There are two accepted ways to deal with the polaron system, variational ansatz method and many-body T -matrix method, which have been proved to be equivalent by Chevy in 2007 [55]. The former is intuitive and has been extended to the dynamic version [56, 57]. Meanwhile, the later is a little more complicated. We need to calculate the self energy perturbatively and then obtain the spectrum function as well as quasiparticle parameters. However, the T -matrix approach can be conveniently constructed by the non-equilibrium GF to give a complete description of the open quantum system taking into account all the effects of the LMEQ without ignoring the quantum jump term [58], which is the method we adopt in this work.

We start from the full partition function of the system,

$$\mathcal{Z} = \int_C D[\bar{c}, c, \bar{f}, f] e^{iS_{\text{imp}} + iS_{\text{bath}} + iS_{\text{int}}}, \quad (3)$$

where C is the Keldysh integral contour. Performing the Fermi Keldysh rotation, the bare impurity action reads

$$S_{\text{imp}} = \sum_k \bar{c}_\mu(k) G_{0,c}^{-1, \mu\nu}(k) c_\nu(k), \quad (4)$$

where the $\mu, \nu = 1, 2$ are Keldysh indices and the Einstein summation convention of repeated indices is connoted here and thereafter. The matrix of $G_{0,c}^{-1}$ is upper

triangular, so we can straightforwardly read out the bare retarded and advanced GFs

$$G_{0,c}^{R/A}(\mathbf{k}, \omega) = [\omega - \varepsilon_c(\mathbf{k}) \pm i0^+]^{-1}. \quad (5)$$

According to the fluctuation-dissipation relation (FDR) for steady state, the bare Keldysh GF can always be expressed with the corresponding retarded and advanced GFs ,

$$G_{0,c}^K(\mathbf{k}, \omega) = F_c^{eq}(\omega)[G_{0,c}^R(\mathbf{k}, \omega) - G_{0,c}^A(\mathbf{k}, \omega)]. \quad (6)$$

In the impurity limit, where the density of impurity atoms is vanishing small, we have $F_c^{eq} = 1$.

The GFs for the bath are some complicated. The retarded, advanced and Keldysh GFs should be obtained simultaneously by reverting the matrix of $G_{0,f}^{-1}$, which can be extracted from the dissipative bath action with a Keldysh rotation applied (see Appendix).

$$G_{0,f}^{R/A}(\mathbf{k}, \omega) = [\omega - \varepsilon_c(\mathbf{k}) \pm \frac{i\gamma(\mathbf{k})}{2}]^{-1}, \quad (7)$$

$$G_{0,f}^K(\mathbf{k}, \omega) = F_{0,f}(\mathbf{k}, \omega)[G_{0,f}^R(\mathbf{k}, \omega) - G_{0,f}^A(\mathbf{k}, \omega)], \quad (8)$$

where the distribution function $F_{0,f}(\mathbf{k}, \omega) = 1 - 2\eta(\mathbf{k})$ and $\eta(\mathbf{k}) = \Omega(\mathbf{k})/\gamma(\mathbf{k})$ is the average particle number for momentum \mathbf{k} .

Next, we introduce an auxiliary molecular field Δ to decouple the four-operator interaction term in the total action. By performing a Hubbard-Stratonovich transformation, the interaction part of the action becomes

$$S_{\Delta,c,f} = \int_C dx (-\bar{\Delta} f c - \bar{c} f \Delta), \quad (9)$$

and further changes into

$$S_{\Delta,c,f} = - \int dx \frac{1}{\sqrt{2}} (f_\mu \bar{\Delta}_a \gamma_{\mu\nu}^a \sigma_{\nu\eta}^x c_\eta + \text{h.c.}), \quad (10)$$

with a successive Keldysh rotation to achieve a basis transformation, where $\mu, \nu, \eta = 1, 2$, and $a = q, cl$ are fermion and boson Keldysh indices respectively. The elements of γ^a are $\gamma^{cl} = I$ and $\gamma^q = \sigma^x$, where I is the identity matrix and σ^x is the x component of Pauli matrices. To calculate the self-energy, we integrate out the fermionic bath degrees of freedom and obtain the induced interaction action for molecule and impurity,

$$S_{\Delta,c} = -\frac{1}{2} \int dx dx' \bar{\Delta}_a(x) \gamma_{\mu\nu}^a \sigma_{\nu\eta}^x c_\eta(x) G_{0,f}^{\mu\tau}(x, x') \times \bar{c}_\alpha(x') \sigma_{\alpha\beta}^x \gamma_{\beta\tau}^b \Delta_b(x'). \quad (11)$$

Under the framework of non-self-consistent T -matrix method [54], accurate to first order, the real space self-energy of the molecule and impurity are solved out as,

$$\Sigma_{\Delta}^{ab}(x, x') = \frac{i}{2} \gamma_{\mu\nu}^a \sigma_{\nu\eta}^x G_{0,f}^{\mu\tau}(x, x') G_{0,c}^{\eta\alpha}(x, x') \sigma_{\alpha\beta}^x \gamma_{\beta\tau}^b, \quad (12)$$

for molecule, and

$$\Sigma_c^{\alpha\eta}(x, x') = \frac{i}{2} \sigma_{\alpha\beta}^x \gamma_{\beta\tau}^b G_{\Delta}^{ba}(x', x) G_{0,f}^{\mu\tau}(x', x) \gamma_{\mu\nu}^a \sigma_{\nu\eta}^x. \quad (13)$$

the self-energy of molecule and impurity can be expressed by the corresponding retarded, advanced and Keldysh GFs respectively.

C. The retarded self-energy and spectrum function

To obtain the spectrum functions and quasiparticle parameters, we need to get the GFs of molecule and impurity, which is essentially to obtain the corresponding retarded self-energy. In the steady state, the system is time- and space-translational invariant, so all the real-space GFs and self-energy can be written out by their Fourier transforms for the relative coordinates, which is more convenient to discuss the quasiparticle properties. Setting $a = q$ and $b = cl$ in Eq. (12) and taking the Fourier transform, we obtain the momentum-space retarded self-energy of the molecule state,

$$\Sigma_{\Delta}^R(q) = \frac{i}{2V} \sum_{p_1} \left\{ G_{0,f}^R(q - p_1) G_{0,c}^K(p_1) + G_{0,f}^K(q - p_1) G_{0,c}^R(p_1) \right\}. \quad (14)$$

Performing the contour integral for frequency, the retarded self-energy of molecule becomes

$$\Sigma_{\Delta}^R(q) = \frac{1}{V} \sum_{\mathbf{p}_1} \frac{1 - \eta(\mathbf{p}_1)}{\omega - \varepsilon_f(\mathbf{p}_1) - \varepsilon_c(\mathbf{q} - \mathbf{p}_1) + i\frac{\gamma(\mathbf{p}_1)}{2}}, \quad (15)$$

and the retarded GF of molecule is written as

$$G_{\Delta}^R(\mathbf{q}, \omega) = \frac{1}{\frac{1}{g} - \Sigma_{\Delta}^R(\mathbf{q}, \omega) + i0^+}. \quad (16)$$

Following the similar procedure, the retarded self-energy of impurity is expressed as

$$\begin{aligned} \Sigma_c^R(k) &= -\frac{i}{2V} \sum_{p_1} G_{\Delta}^K(k_+) G_{0,f}^A(p_1) + G_{\Delta}^R(k_+) G_{0,f}^K(p_1) \\ &= \frac{1}{V} \sum_{\mathbf{p}_1} \eta(\mathbf{p}_1) G_{\Delta}^R(\mathbf{p}_1 + \mathbf{k}, \varepsilon_f(\mathbf{p}_1) + \omega), \end{aligned} \quad (17)$$

where $k_+ = p_1 + k$. Then the retarded GF of the impurity is given by

$$G_c^R(k) = \frac{1}{\omega - \varepsilon_c(\mathbf{k}) - \Sigma_c^R(k) + i0^+}. \quad (18)$$

The spectrum functions of molecule and impurity are written as

$$A_{\Delta}(q) = -\frac{1}{\pi} \text{Im}[G_{\Delta}^R(q)], \quad (19)$$

$$A_c(k) = -\frac{1}{\pi} \text{Im}[G_c^R(k)]. \quad (20)$$

The pole of the retarded GF of impurity determines the polaron energy, that is

$$E_p(\mathbf{k}) = \varepsilon_c(\mathbf{k}) + \text{Re}\Sigma_c^R(\mathbf{k}, E_p). \quad (21)$$

For our system, E_p always increases as $|\mathbf{k}|$ on the raise, so only the solutions at zero momentum are considered and the equation above develops into $E_p = \text{Re}\Sigma_c^R(0, E_p)$. According to Landau Fermi liquid theory, a polaron state behaves like a quasiparticle with collective energy shift E_p , residue Z , effective mass m_c^* , and the two-body decay rate γ_+ , so the asymptotic behavior of the GF in the zero momentum limit takes the form

$$G_c^R(\mathbf{k}, \omega) = \frac{Z}{\omega - \frac{\hbar^2 \mathbf{k}^2}{2m_c^*} - E_p + i\gamma_+}. \quad (22)$$

Expanding the retarded self-energy in Eq. (18) to first order at the pole and Comparing the GF with that in Eq. (22), we have

$$Z = \frac{1}{1 - \frac{\partial \text{Re}\Sigma_c^R(0, \omega)}{\partial \omega} |_{\omega=E_p}}, \quad (23)$$

$$\frac{m_c^*}{m_c} = \frac{1 - \frac{\partial \text{Re}\Sigma_c^R(0, \omega)}{\partial \omega} |_{\omega=E_p}}{1 + \frac{\partial \text{Re}\Sigma_c^R(\varepsilon_c(\mathbf{k}), E_p)}{\partial \varepsilon_c(\mathbf{k})} |_{k=0}}, \quad (24)$$

$$\gamma_+ = -2Z \text{Im}\Sigma_c^R(0, E_p). \quad (25)$$

For two-dimensional Fermi gases, the above bare interaction strength g should be renormalized by the two-body binding energy E_B as

$$\frac{1}{g} = - \sum_k \frac{1}{E_B + \varepsilon_r}, \quad (26)$$

where $\varepsilon_r = \frac{\hbar^2 k^2}{2m_r}$, and $m_r = \frac{m_c m_f}{m_c + m_f}$ is the reduced mass.

III. NUMERICAL RESULTS AND DISCUSSION

A. Dressed molecule state

The molecular state plays an vital role in the scenario of the interaction between the impurity and the bath, not only because the introduction of auxiliary field can easily decouple the interaction potential, but also because its retarded GF is just the T -matrix characterizing the moving impurity scattered by the bath fermions. From the formula derived above, we could conclude that all the GFs depend on the $\gamma(\mathbf{k})$ and the ratio of $\eta(\mathbf{k}) = \Omega(\mathbf{k})/\gamma(\mathbf{k})$. For simplicity, we limit the driving and dissipation to the same range depicted by a cutoff momentum k_r , within which both the $\gamma(\mathbf{k}) = \gamma_0$ and $\eta(\mathbf{k}) = \eta$ are nonzero constants and zero elsewhere. In addition, unless otherwise specified, we set $m_c = m_f = 1/2$ and $k_F = 1$ in the calculations below.

We start by analysing the parameter regime where the dissipation is vanishing small. On this condition, the

self-energy of the molecular field can be separated into two parts as $\Sigma_\Delta^R = \Sigma_\Delta^{R,1} + \Sigma_\Delta^{R,2}$, where the first part is $\Sigma_\Delta^{R,1} = 1/V \sum_{\mathbf{p}_1} 1/[(\omega - \varepsilon_f(\mathbf{p}_1) - \varepsilon_c(\mathbf{q} - \mathbf{p}_1) + i0^+)]$ and the second part is $\Sigma_\Delta^{R,2} = -\eta/V \sum_{|\mathbf{p}_1| < k_r} 1/[\omega - \varepsilon_f(\mathbf{p}_1) - \varepsilon_c(\mathbf{q} - \mathbf{p}_1) + i0^+]$. Here, we only focus on the molecular bound state, so the energy must be less than the kinetic energy of the center of mass of a molecule, that is $\omega < \min_{\mathbf{p}_1} [\varepsilon_f(\mathbf{q}/2 + \mathbf{p}_1) + \varepsilon_c(\mathbf{q}/2 - \mathbf{p}_1)] = q^2/2M$. In this case, the two integrands in $\Sigma_\Delta^{R,1}$ and $\Sigma_\Delta^{R,2}$ do not have imaginary parts. Setting the upper limit of integral of \mathbf{p}_1 to Λ in $\Sigma_\Delta^{R,1}$, we conclude that

$$\Sigma_\Delta^{R,1} = -\frac{1}{8\pi} \ln \left| \frac{\frac{\Lambda^2}{\tilde{\mu}} - \tilde{\omega} + u_q}{u_q - \tilde{\omega}} \right|, \quad (27)$$

where we have used the notations $\tilde{\mu} = k_r^2$, $x = p_1^2/\tilde{\mu}$, $\tilde{\omega} = \omega/(2\tilde{\mu})$, $\omega_q^* = q^2/2M$ and $u_q = \omega_q^*/(2\tilde{\mu})$ to simplify the expression above. In the meantime, the $\Sigma_\Delta^{R,2}$ evolves into

$$\Sigma_\Delta^{R,2} = \int_0^1 dx \int_0^{2\pi} d\theta \frac{\eta/(16\pi^2)}{x + 2u_q - \tilde{\omega} - 2\sqrt{xu_q} \cos \theta}. \quad (28)$$

Using the integral identity

$$\int_0^{2\pi} d\theta \frac{1}{a + b \cos \theta} = \frac{\pi \text{sign}(a) \Theta(a^2 - b^2)}{\sqrt{a^2 - b^2}}, \quad (29)$$

we can figure out the second part of retarded self-energy of the molecular field and then obtain the inverse of the retarded GF of the molecular field

$$G_\Delta^{R,-1}(\mathbf{q}, \omega) = \frac{1}{g} - \Sigma_\Delta^R(\mathbf{q}, \omega) = \frac{1}{8\pi} \ln \left| \frac{E_B/(2\tilde{\mu})}{u_q - \tilde{\omega}} \right| - \frac{\eta}{16\pi} \ln \left[\frac{\sqrt{\frac{(\tilde{\omega}-1)^2}{4} + u_q(u_q - \tilde{\omega})} - \frac{\tilde{\omega}-1}{2}}{u_q - \tilde{\omega}} \right]. \quad (30)$$

Solving the pole of $G_\Delta^R(\mathbf{q}, \omega)$, we can obtain the molecular bound state shown as the black dashed lines in Fig. (1) (a)-(d), which are in accord with the corresponding numerical results obtained under small γ_0 and the same other parameters. It is interesting that the gap between the boundary of molecule-hole continuum and the molecular bound state decreases when the dissipation cutoff momentum k_r is on the raise, which can be understood by the composition of retarded self-energy when the dissipation is infinitesimal. In this instance, $\Sigma_\Delta^{R,1}$ is the self-energy of the vacuum scattering (impurity scatters with a single bath fermion) without dissipation. $\Sigma_\Delta^{R,2}$ comes from a finite density of bath gases, which represents the contribution of dissipative bath fermions to the self-energy by participating in the formation of molecular state. For the vacuum scattering, the T -matrix is known as

$$T_0^{-1}(\mathbf{q}, \omega) = -\frac{m_r}{2\pi} \left[\ln \left(\frac{E}{E_B} \right) - i\pi \right], \quad (31)$$

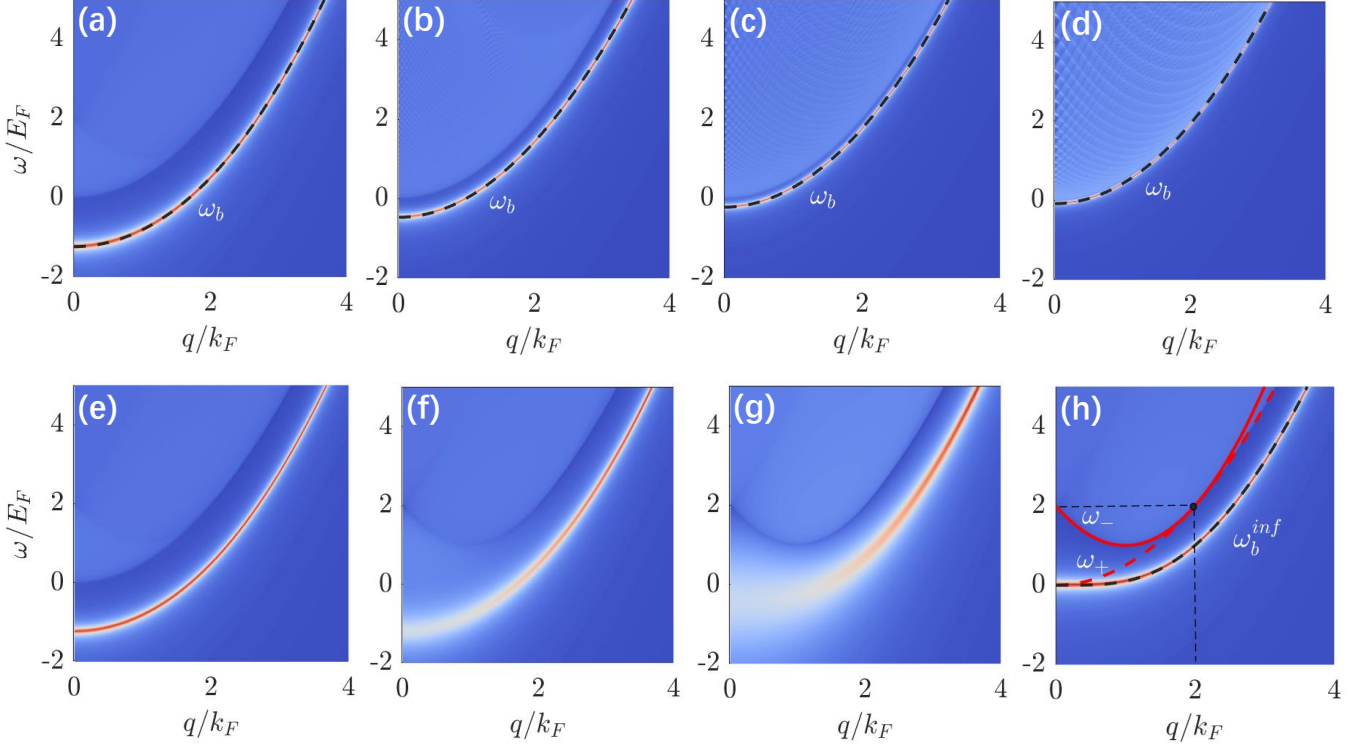


FIG. 1. (Color online) Molecular spectral function A_Δ with different dissipation cutoff momentum k_r [(a), $k_r/k_F = 1.0$; (b), $k_r/k_F = 2.0$; (c), $k_r/k_F = 3.0$; (d), $k_r/k_F = 5.0$] for a small loss rate $\gamma_0/E_F = 0.01$, and with different dissipation strength γ_0 [(e), $\gamma_0/E_F = 0.01$; (f), $\gamma_0/E_F = 1.0$; (g), $\gamma_0/E_F = 5.0$; (h), $\gamma_0/E_F = 30$] for $k_r/k_F = 1.0$. Other parameters are $\eta = 0.5$, $E_B/E_F = 2$. In addition, the black dashed lines in (a)-(d) are the analytical results of molecular bond state ω_b with $\gamma_0 = 0^+$ and the same other parameters in their respective subplots, which are in perfect agreement with the numerical results at small γ_0 . In (h), we show the analytical solution of the lower bound of molecule-hole continuum at infinit dissipation marked by ω_- (red solid line) and ω_+ (red dashed line) to the left and right of their intersection (black dot) respectively (A detailed explanation is provided later in this section). Meanwhile, the ω_b^{inf} (black dashed line) illustrates the analytical solution of molecular bound state under the same conditions. These analytical results are also in line with the numerical results at large γ_0 .

where $E = \omega - \mathbf{q}^2/2M + i0^+$ and $M = m_c + m_f$. It is clear that T_0 has a pole at $\omega^0 = \mathbf{q}^2/2M + i0^+ - E_B$. When the background participates in the scattering process, the equation of bound state energy develops into

$$T_0^{-1}(\mathbf{q}, \omega^*) = \Sigma_{\Delta}^{R,2}(\mathbf{q}, \omega^*). \quad (32)$$

Since the energy of bound state must be less than kinetic energy of center of mass, then we obtain immediately that $\ln[(\omega^0 - \mathbf{q}^2/2M)/(\omega^* - \mathbf{q}^2/2M)] > 0$, claiming $\omega^* > \omega_0$. Moreover, the right hand side of Eq. (32) grows monotonically with k_r , so as the ω^* , which explains why the gap between the energy of bound state and that of boundary of molecule-hole continuum narrows with k_r .

In the presence of dissipation, the molecular bound state shows obvious non-monotonic behavior. Under moderate dissipation strength, the spectral function presents a certain degree of broadening, as shown in Fig. 1(f), (g). However, it becomes well defined again, when γ_0 grows to a large enough value, e.g., $\gamma_0 = 30E_F$ as shown in Fig. 1(h), indicating the revival of bound

state. It is that the competition between the increase of argument of the self-energy by the growth of dissipation and the decrease of its modulus by the same reason prompts this non monotonicity. For each channel within k_r , when the dissipation increases slightly from zero, the imaginary part of the self-energy increases significantly, which is particularly obvious for small momentum channels. However, when the dissipation is soaring, the contribution of the summation terms to the self-energy in all the dissipative channels will eventually be suppressed by the divergent denominator in Eq. (15), resulting in the attenuation of all the channels within k_r .

Especially, if γ_0 is infinite, the retarded molecular self-energy is given by

$$\Sigma_{\Delta}^R(\mathbf{q}, \omega) = \sum_{|\mathbf{p}_1| > k_r} \frac{1/V}{\omega - \varepsilon_f(\mathbf{p}_1) - \varepsilon_c(\mathbf{q} - \mathbf{p}_1) + i0^+} \quad (33)$$

In this limit, the dissipative boundary takes a similar role as the Fermi surface. In other words, effective ‘‘Pauli blocking’’ is reproduced in this situation where the T -

matrix develops into

$$T(q, \omega) = T_0 \left(\frac{z}{2} \pm \frac{1}{2} \sqrt{(z - \varepsilon_f)^2 - 4\varepsilon_f(q) \frac{k_r^2}{2m}} \right), \quad (34)$$

specifying $z = \omega - \frac{\hbar^2 k_r^2}{2m_r} + i0^+$, and $\pm = \text{sign}\{\text{Re}[z - \varepsilon_f(q)]\}$. Proceed to the next step, we analytically solve the dispersion of the bound state out as

$$\omega_b^{inf}(\mathbf{q}) = \frac{\frac{1}{4}\varepsilon_f(\mathbf{q})(\varepsilon_f(\mathbf{q}) - 4\frac{k_r^2}{2m}) - E_b^2}{E_B + \frac{1}{2}\varepsilon_f(\mathbf{q})} + \frac{k_r^2}{2m_r}, \quad (35)$$

which is plotted in Fig. 1(h) with black dashed line and is very consistent with the numerical result under large γ_0 . Meanwhile, it is the minimum value of $\frac{q^2}{2M} + \frac{p_1^2}{m}$ with the confinement $|\frac{\mathbf{q}}{2} + \mathbf{p}_1| > k_r$ that determine the threshold of the molecule-hole continuum. This optimization problem needs to be discussed in different situations. On the one hand, if $k_r < \frac{q}{2}$, then $\omega_+(q) = \frac{q^2}{2M}$; on the other hand, if $k_r > \frac{q}{2}$, then $\omega_-(q) = \frac{(q - k_r)^2 + k_r^2}{2m}$. The two curves intersect at the $(2k_r, 2k_r^2)$ as shown in Fig. 1(h). When the dissipation is infinite, the behavior of molecular state is the same as that in the scattering of impurity and Fermi sphere. In fact, this phenomenon can also be interpreted as a Zeno effect, where the dissipation processes can be viewed as continuous measurement [54]. A similar scenario has been found by Ueda et.al.[59] in a non-Hermitian BCS superfluid with complex-valued interaction, which is due to inelastic scattering between fermions. In their work, the superfluid gap never collapses but it is enhanced by the dissipation as a result of Zeno effect. Actually, in the impurity limit, our molecular bound state can be viewed as a counterpart of the population-balanced Fermi superfluid state.

We further characterize the scattering by analyzing the phase of the T -matrix. We start from the scenario in the absence of dissipation. In the case of vacuum scattering where $\eta = 0$, the many-body dynamics reduces to a two-body one. The aforementioned dispersion of the pole of T_0 , i.e. ω_0 , generates an excitation with energy $-E_B$ at zero momentum, which is confirmed by a sharp peak and a π jump, in the process of crossing the energy of bound state, in Fig. 2(a1) and (a2) respectively with red dotted lines. The phase is zero in the regime without state, i.e. $\omega < -E_B$, and jump to π when crossing the poles of bound states, i.e. $\omega = -E_B$. It maintains this value within the gap between bound and continuous regime and then begins to decay monotonically when $\omega > 0$ in that the continuous state emerges. If η is more than zero, the bath states within k_r have a certain probability of being occupied, then on average there is a finite density of bath gases. Therefore, the formation of dressed molecular state is more inclined to deduct the bath states within k_r , resulting in a blueshift of bound state energy, as shown in Fig. 1(e) with blue dashed line whilst consistent with Fig. 2(b1). It is noted that although the continue state still arises at $\omega = 0$, which is the minimum of total kinetic energy of a molecule without any

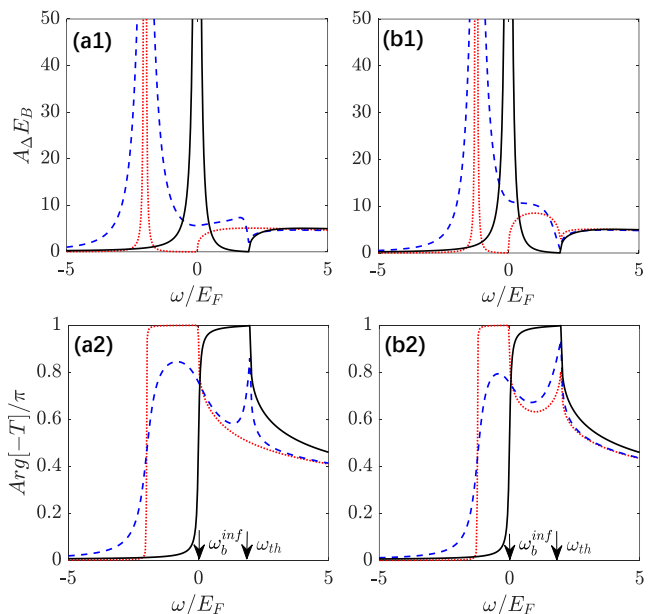


FIG. 2. (Color online) Spectrum function of the molecular bond state at zero momentum, i.e. $A_\Delta(0, \omega)E_B$ and the phase of the T -matrix, i.e. $\text{Arg}[-T]/\pi$ for different average particle number [(a1), (a2), $\eta = 0$; (b1), (b2), $\eta = 0.5$] and different dissipation [$\gamma_0 = 0$: dotted red line; $\gamma_0 = E_F$: dashed blue line; $\gamma_0 = 30E_F$: black solid line] as a function of energy. The arrow indicate the bound state $\omega_b^{inf} = 0E_F$ and the threshold of the continue state $\omega_{th} = 2E_F$ for infinite loss rate case. In all the subplots, we have set $m_c = m_f$, $E_B = 2E_F$ and $k_r = k_F$ in the calculation.

constraints, the phase shows non monotonicity and has a peak at $\omega > 0$ (see details below).

When dissipation is applied to the background gas, the spectral function of bound state exhibits greater broadening and blueshift than its corresponding lossless case. Meanwhile, the T -matrix in the gap regime is no longer a real one due to the finite dissipation, resulting in the π platform evolves into a broad peak (shown as blue dashed line in Fig. 2(a2) and (b2)). Interestingly, whether the dissipation or the average particle number is not zero, the phase of T -matrix is non monotonic in the continuous regime, especially their peaks are in the same position which coincides with that where the continuous state begins to emerge when the dissipation is infinite. This commonality is due to the fact that the final effect is to reconstruct the same “Fermi surface” no matter increasing the dissipation strength or increasing the average number of particles. In their respective limit cases, the effective “Pauli blocking” will push the threshold of continuous state to the optimal value obtained in the subspace: $k_f > k_r$.

The numerical solutions with very large dissipation are also shown by black solid lines in Fig. 2 for comparison with the analytical results with infinite dissipation. It’s clear from the Eq. (35) that the bound state at zero

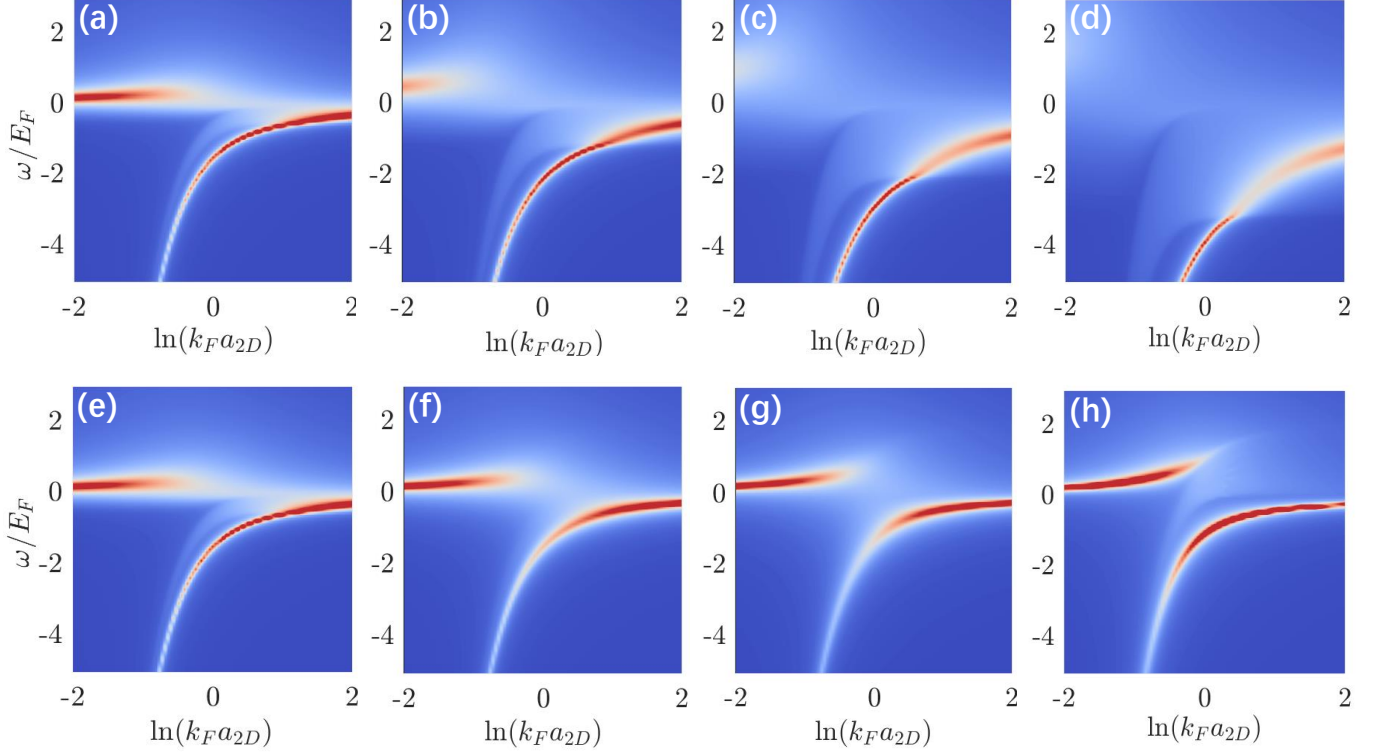


FIG. 3. (Color online) Polaron spectral function, i.e. $A_c(p=0, \omega)$ as a function of interaction strength parameter, i.e. $\ln(k_F a_{2D})$ with different k_r [(a), $k_r/k_F = 1.0$; (b), $k_r/k_F = 1.5$; (c), $k_r/k_F = 2.0$; (d), $k_r/k_F = 2.5$] for $\gamma_0 = 0.1E_F$, and with different γ_0 [(e), $\gamma_0/E_F = 0.1$; (f), $\gamma_0/E_F = 1.0$; (g), $\gamma_0/E_F = 5.0$; (h), $\gamma_0/E_F = 30$] for $k_r/k_F = 1.0$. The average particle number is $\eta = 0.5$.

momentum is $\omega_b^{inf} = \frac{\hbar^2 k_r^2}{2m_r} - E_B$, no matter η is zero or finite, which is just at the position of phase jump of the corresponding numerical results. To address the threshold of continue state, we make use of the condition that the bath atom can not be scattered into the dissipation subspace: $k_f < k_r$. The momentum of bath atom is written as $\mathbf{k}_f = \frac{m_f}{M} \mathbf{q} - \mathbf{k}_{rel}$, where \mathbf{q} is the center of mass momentum and \mathbf{k}_{rel} is the relative momentum. Then, the effective ‘‘Pauli blocking’’ requires

$$|\sqrt{2m_r E_{rel}} - \frac{m_f}{M} q| > k_r, \quad (36)$$

that is $E_{rel} > \omega_{th} - \frac{\hbar^2 q^2}{2M} = \frac{(k_r + \frac{m_f}{M} q)^2}{2m_r}$. Here the ω_{th} at $\mathbf{q} = 0$ shows no difference with the outcomes of numerical simulation with large dissipation, e.g., $\gamma_0 = 30E_F$.

B. Polaron state

In our system, the impurity does not directly participate in the nonunitary evolution, but it is affected by dissipation through the scattering with the intermediate molecular state. In this section, we mainly concern the minimal energy state of polarons that occur at $\mathbf{k} = 0$. We can intuitively observe the excitations due to the spectral

function of impurity, the resonant peaks of which correspond to polaron states. In Fig. (3), we connect E_B with a_{2D} by $E_B = 1/ma_{2D}^2$ [29], and present the contour plot of $A_c(\mathbf{k}=0, \omega)$. For small γ_0 and $k_r = k_F$, the attractive branch is well-defined with weak interaction. When the interaction increases, a repulsive polaron emerges and the spectrum weight transfers from the attractive polaron to repulsive polaron. Finally the repulsive polaron becomes long-lived and stable with large interaction. This scenario is basically the same as when the background gases has Fermi surface [29]. The polaron spectral function shows that they first diffuse and converge with the increase of dissipation (see second row in Fig. (3)), which can be attributed to the Zeno effect, as mentioned in the previous section. When the k_r exceeds k_F , the dissipation will affect the higher energy excitations, which can be corroborated from the obvious weakening of the repulsive polaron in Fig. 3(b), (c), and (d) (see explanations below). In addition, the molecule-hole continuum spread out more with the increase of k_r .

We can see the different responses of the two excitations to k_r more clearly from the frequency sweep with a fixed E_b in Fig. (4)(a). The attractive and the repulsive polarons show different behaviors as k_r on the raise: although the energies of both of them are red-shifted, the spectral signal of the former is enhanced due

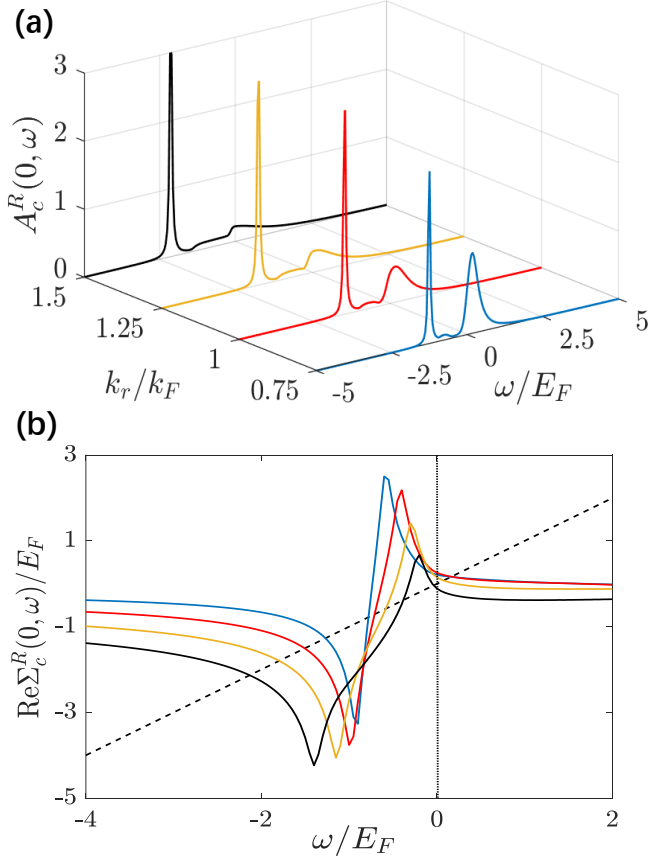


FIG. 4. (Color online) Polaron spectral function (a) and self-energy (b) with different k_r [$k_r/k_F = 0.75$: blue line; $k_r/k_F = 1.0$: red line; $k_r/k_F = 1.25$: yellow line; $k_r/k_F = 1.5$: black line;]. Other parameters are: $E_B = 2E_F$, $\gamma_0 = 0.1E_F$, and $\eta = 0.5$. The dashed black line is the function of $g(\omega) = \omega$.

to the weakening of the latter. On the one hand, these frequency shifts in common can be confirmed by calculating the positions of polaron states, which are obtained by solving the Eq. (21) for $\mathbf{k} = 0$ in our treatment (see the intersections of the straight dashed line $g(\omega) = \omega$ and self-energy curves in Fig. (4)(b)). On the other hand, k_r acts as Fermi surface to some extent. In this picture, the particle-hole excitations around it dominate the formation of polarons. Therefore, with the increase of k_r , the repulsive polaron is easier to couple with the virtual molecular state, that is, it will be more dissipated. Meanwhile, the attractive branch becomes more and more like a bare impurity, which is reflected in the increase of two-body decay and the decrease of effective mass, as shown in Fig. (5)(c) and (d). As a result, the spectral weight of the repulsive polaron is continuously shifted to that of the attractive one.

To further describe the properties of attractive polaron and compare them with the case without dissipation (at this time, the lifetime of attractive polaron is infinite, i.e. $\gamma_+ = 0$), we present polaron energy, quasi-particle residue, effective mass and two-body de-

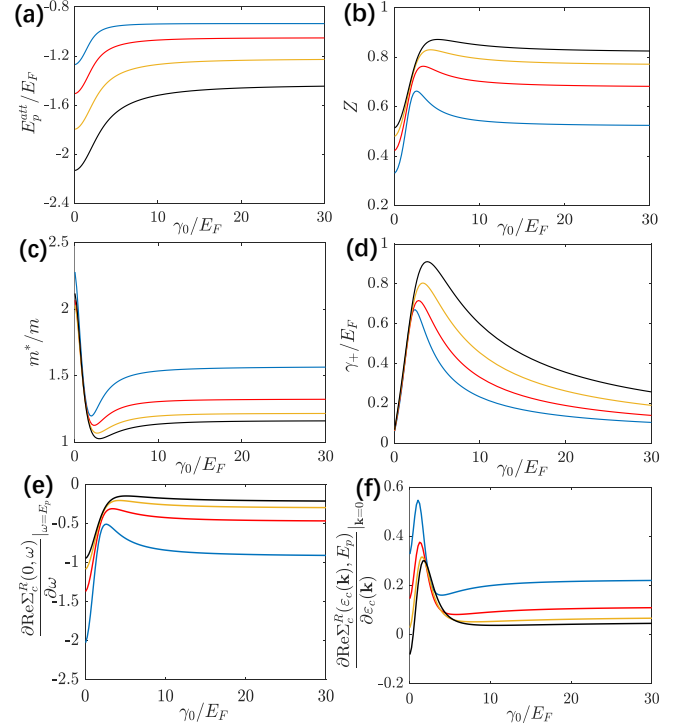


FIG. 5. (Color online) Quasiparticle parameters and partial derivatives vs γ_0 . Each color represents the same k_r as in Fig. 4, so do η and E_b .

causing rate as functions of γ_0 for mass balance case in Fig. (5). These quantities all initially change vs γ_0 and gradually reach their saturation values respectively, which should be explained by the Zeno effect as in the previous section. The polaron energy displays redshift for specific γ_0 with added k_r showing consistence with Fig. (4). The quasiparticle ratio Z , effective mass m_c^*/m_c and two-body decay γ_+ show nonmonotonic behavior vs γ_0 . The trend change positions of the three curves are basically the same, and they are all at the dissipation of moderate intensity, i.e. $\gamma_0/E_F \sim 2$ for our setup. In order to understand these results more clearly, we exhibit two partial derivatives $\partial \text{Re}\Sigma_c^R(0, \omega)/\partial \omega|_{\omega=E_p}$ and $\partial \text{Re}\Sigma_c^R(\varepsilon_c(\mathbf{k}), E_p)/\partial \varepsilon_c(\mathbf{k})|_{\mathbf{k}=0}$ in Fig. (5)(e) and (f). Then, based on Eq. (23) and (24), the behaviors of Z and m^*/m are unambiguous. These results are consistent with our point of view in this paper, that is, only moderate dissipation is detrimental to the formation of polarons. Since only the bath will be dissipated, when $\gamma_0 \sim E_b$, the properties of the system are as follows: 1) The proportion of impurity excitation in polaron goes up; 2) The effective mass approaches unit; 3) The lifetime of polaron is greatly compressed. These results are helpful for us to observe attractive polaron in a dirty environment, e.g., a background gas strongly coupled with itself environment.

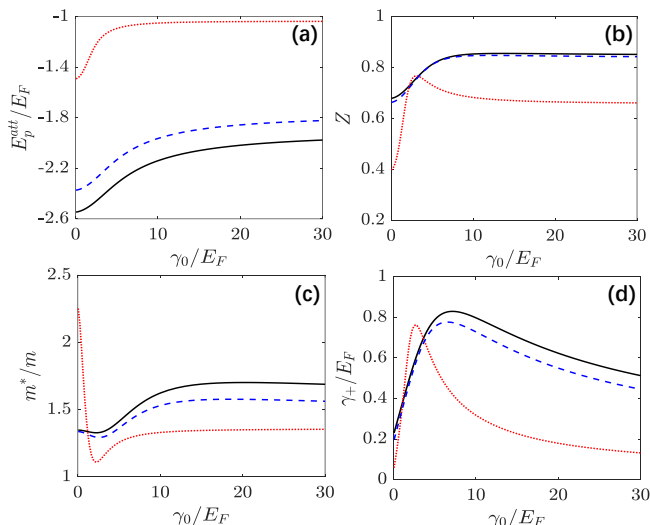


FIG. 6. (Color online) Polaron energy, residue, effective mass, and two-body decay as a function of the dimensionless loss rate γ_0/E_F for the mixture of ${}^6\text{Li}$ - ${}^{40}\text{K}$ (black solid line), ${}^7\text{Li}$ - ${}^{40}\text{K}$ (blue dashed line) and ${}^7\text{Li}$ - ${}^6\text{Li}$ (red dashed line). The other parameters are set as $E_B = 2E_F$, $k_r = k_F$ and $\eta = 0.5$.

C. Experimental relevance

Finally, we demonstrate the quasiparticle properties of the experiment realizable systems. Since the impurity is a single atom, either a Bose or Fermi impurity can be a candidate. Here, we consider one kind of Fermi-Fermi and two kinds of Bose-Fermi mixtures as shown in Fig. (6). In the small impurity density limit, the quasiparticle properties of the minority can be detected by RF spectrum or Raman spectrum.

Comparing with the three kinds of experimental candidates, there is a distinct change for the case with closer mass of impurity and bath atom in terms of quasiparticle properties when we tune the loss rate. So a mixture of minority ${}^7\text{Li}$ and majority ${}^6\text{Li}$ turn to be a more desirable candidate for us to manipulate polaron state by controlling the dissipation strength.

IV. CONCLUSION AND OUTLOOK

In summary, we use non-self-consistent T -matrix theory to solve the polaron problem in a driven-dissipative bath. Non-equilibrium Green's function is adopted to include the effect of the quantum jump term in the LMEQ.

We illustrate the non-trivial interplay among dissipation range, dissipation strength, as well as interaction. In particular, there are two analytic results: 1) we elucidate the mechanism that the gap between molecular state and molecule-hole continuum decreases monotonically with the dissipation range when the dissipation strength is very small. 2) we obtain the dispersion of bound state as a function of interaction strength and dissipation range when the dissipation strength is infinit large, which is independent of the average number of particles in the background medium. We numerically demonstrate the molecular and polaron spectrum functions with different dissipation strength, and find that their resonant peaks become diffuse only under moderate dissipation, indicating the quasiparticles cease to exist in this regime. Meanwhile, the positions of both the attractive and repulsive polarons display redshift when the dissipation range increases, and the two polarons exhibit opposite behavior in this process: we see an increment and a decrement of the weights of attractive and repulsive polarons respectively. We also calculate the quasiparticle parameters vs dissipation strength with different dissipation ranges for the attractive polaron. The residue, effective mass and two-body decay show nonmonotonic characters due to the interplay between the intrinsic energy scale of the system and the measurement frequency from the environment (understanding dissipation from another perspective). However, they eventually tend to their respective saturation values in the quantum-Zeno limit, i.e. $\gamma_0 = \infty$. Our model can be implemented in recent experiments [47–50], and the results in this work can help us to find appropriate setups in dissipative cold atom experiments to observe clear-cut polaron signals.

Based on the technical methods used in this work, we can further study the experimental realizable system, e.g., the exciton-polariton system in quantum wells embedded in an optical micro cavity. The leakage of photons from the cavity and the decay of exciton via radiative and non-radiative processes make the platform a natural open quantum system [61–63]. How to use nonequilibrium Green's function to characterize natural open systems is reserved for future research.

V. ACKNOWLEDGMENT

Y.C. was supported by the NSFC-China (Grants No. 11704029 and No. 12174024). J.Z. was supported by the NSFC-China (Grants No. 11504038). The authors acknowledge stimulating discussions with Hui Hu and Jia Wang.

-
- [1] L. D. Landau, Phys. Z. Sowjetunion, über Die Bewegung der Elektronen in Kristallgitter **3**, 644 (1933).
 [2] P. A. Lee, N. Nagaosa, and X.-G. Wen, Doping a Mott insulator: Physics of high-temperature superconductivity,

- Rev. Mod. Phys. **78**, 17 (2006).
 [3] N. Mannella, W. L. Yang, X. J. Zhou, H. Zheng, J. F. Mitchell, J. Zaanen, T. P. Devereaux, N. Nagaosa, Z. Hussain, and Z.-X. Shen, Nodal quasiparticle in pseu-

- dogapped colossal magnetoresistive manganites, *Nature (London)* **438**, 474 (2005).
- [4] G. Baym and C. Pethick, *Landau Fermi-Liquid Theory: Concepts and Applications*, 1st ed. (Wiley-VCH, New York, 1991).
- [5] M.E. Gershenson, V. Podzorov, and A.F. Morpurgo, Colloquium: Electronic transport in single-crystal organic transistors, *Rev. Mod. Phys.* **78**, 973 (2006).
- [6] I. Bloch, J. Dalibard, and W. Zwerger, Many-body physics with ultracold gases, *Rev. Mod. Phys.* **80**, 885 (2008).
- [7] C. Chin, R. Grimm, P. Julienne, and E. Tiesinga, Feshbach resonances in ultracold gases, *Rev. Mod. Phys.* **82**, 1225 (2010).
- [8] A. Schirotzek, C.-H. Wu, A. Sommer, and M.W. Zwierlein, Observation of Fermi polarons in a tunable Fermi Liquid of Ultracold atoms, *Phys. Rev. Lett.* **102**, 230402 (2009).
- [9] Y. Zhang, W. Ong, I. Arakelyan, and J.E. Thomas, Polaron-Polaron Transitions in the Radio-Frequency Spectrum of a Quasi-Two-Dimensional Fermi Gas, *Phys. Rev. Lett.* **108**, 235302 (2012).
- [10] C. Kohstall, M. Zaccanti, M. Jag, A. Trenkwalder, P. Massignan, G. M. Bruun, F. Schreck, and R. Grimm, Metastability and coherence of repulsive polarons in a strongly interacting Fermi mixture, *Nature (London)* **485**, 615 (2012).
- [11] M. Koschorreck, D. Pertot, E. Vogt, B. Fröhlich, M. Feld, and M. Köhl, Attractive and repulsive Fermi polarons in two dimensions, *Nature (London)* **485**, 619 (2012).
- [12] M. Cetina, M. Jag, R. S. Lous, I. Fritsche, J.T. M. Walraven, R. Grimm, J. Levinsen, M. M. Parish, R. Schmidt, M. Knap, and E. Demler, Ultrafast many-body interferometry of impurities coupled to a Fermi sea, *Science* **354**, 96 (2016).
- [13] M.-G. Hu, M. J. Van de Graaff, D. Kedar, J. P. Corson, E. A. Cornell, and D. S. Jin, Bose polarons in the strongly interacting regime, *Phys. Rev. Lett.* **117**, 055301 (2016).
- [14] N. B. Jørgensen, L. Wacker, K. T. Skalmstang, M. M. Parish, J. Levinsen, R. S. Christensen, G. M. Bruun, and J. J. Arlt, Observation of Attractive and Repulsive polarons in a Bose-Einstein condensate, *Phys. Rev. Lett.* **117**, 055302 (2016).
- [15] F. Scazza, G. Valtolina, P. Massiganan, A. Recati, A. Amico, A. Burchianti, C. Fort, M. Inguscio, M. Zaccanti, and G. Roati, Repulsive Fermi polarons in a resonant mixture of ultracold ${}^6\text{Li}$ Atoms, *Phys. Rev. Lett.* **118**, 083602 (2017).
- [16] Z. Yan, P. B. Patel, B. Mukherjee, R. J. Fletcher, J. Struck, and M. W. Zwierlein, Boiling a unitary Fermi liquid, *Phys. Rev. Lett.* **122**, 093401 (2019).
- [17] Z. Z. Yan, Y. Ni, C. Robens, and M. W. Zwierlein, Bose polarons near quantum criticality, *Science* **368**, 190 (2020).
- [18] G. Ness, C. Shkedrov, Y. Florshaim, O. K. Diessel, J. von Milczewski, R. Schmidt, and Y. Sagi, Observation of a smooth polaron-molecule transition in a degenerate Fermi gas, *Phys. Rev. X* **10**, 041019 (2020).
- [19] F. Chevy, Universal phase diagram of a strongly interacting Fermi gas with unbalanced spin populations, *Phys. Rev. A* **74**, 063628 (2006).
- [20] C. Lobo, A. Recati, S. Giorgini, and S. Stringari, Normal state of a polarized Fermi gas at unitarity, *Phys. Rev. Lett.* **97**, 200403 (2006).
- [21] R. Combescot, A. Recati, C. Lobo, and F. Chevy, Normal state of Highly polarized Fermi gases: simple Many-Body approaches, *Phys. Rev. Lett.* **98**, 180402 (2007).
- [22] N. Prokof'ev and B. Svistunov, Fermi-polaron problem: Diagrammatic Monte Carlo method for divergent sign-alternating series, *Phys. Rev. B* **77**, 020408(R) (2008).
- [23] P. Massignan, G.M. Bruun, and H.T.C. Stoof, Twin peaks in rf spectra of Fermi gases at unitarity, *Phys. Rev. A* **77**, 031601(R) (2008).
- [24] R. Combescot and S. Giraud, Normal state of Highly polarized Fermi gases: full many-body treatment, *Phys. Rev. Lett.* **101**, 050404 (2008).
- [25] M. Punk, P.T. Dumitrescu, and W. Zwerger, polaron-to-molecule transition in a strongly imbalanced Fermi gas, *Phys. Rev. A* **80**, 053605 (2009).
- [26] X. Cui and H. Zhai, Stability of a fully magnetized ferromagnetic state in repulsively interacting ultracold Fermi gases, *Phys. Rev. A* **81**, 041602(R) (2010).
- [27] P. Massignan and G.M. Bruun, Repulsive polarons and itinerant ferromagnetism in strongly polarized Fermi gases, *Eur. Phys. J. D.* **65**, 83 (2011).
- [28] C. J. M. Mathy, M. M. Parish, and D. A. Huse, Trimers, Molecules, and polarons in Mass-imbalanced atomic Fermi gases, *Phys. Rev. Lett.* **106**, 166404 (2011).
- [29] R. Schmidt, T. Enss, V. Pietilä, and E. Demler, Fermi polarons in two dimensions, *Phys. Rev. A* **85**, 021602(R) (2012).
- [30] M. M. Parish and J. Levinsen, Highly polarized Fermi gases in two dimensions, *Phys. Rev. A* **87**, 033616 (2013).
- [31] J. Vlietinck, J. Ryckebusch, and K. Van Houcke, Quasiparticle properties of an impurity in a Fermi gas, *Phys. Rev. B* **87**, 115133 (2013).
- [32] S. P. Rath and R. Schmidt, Field-theoretical study of the Bose Polaron, *Phys. Rev. A* **88**, 053632 (2013).
- [33] E. V. H. Doggen and J. J. Kinnunen, Energy and contact of the one-dimensional Fermi polaron at zero and finite temperature, *Phys. Rev. Lett.* **111**, 025302 (2013).
- [34] W. Li, and S. Das. Sarma, Variational study of polarons in Bose-Einstein condensate, *Phys. Rev. A* **90**, 013618 (2014).
- [35] P. Kroiss and L. Pollet, Diagrammatic Monte Carlo study of a mass-imbalanced Fermi-polaron system, *Phys. Rev. B* **91**, 144507 (2015).
- [36] J. Levinsen, M. M. Parish, and G. M. Bruun, Impurity in a Bose-Einstein Condensate and the Efimov Effect, *Phys. Rev. Lett.* **115**, 125302 (2015).
- [37] H. Hu, A.-B. Wang, S. Yi, and X.-J. Liu, Fermi polaron in a one-dimensional quasiperiodic optical lattice: The simplest many-body localization challenge, *Phys. Rev. A* **93**, 053601 (2016).
- [38] O. Goulko, A.S. Mishchenko, N. Prokof'ev, B. Svistunov, Dark continuum in the spectral function of the resonant Fermi polaron, *Phys. Rev. A* **94**, 061605(R) (2016).
- [39] H. Hu, B. C. Mulkerin, J. Wang, and X.-J. Liu, Attractive Fermi polarons at nonzero temperatures with a finite impurity concentration, *Phys. Rev. A* **98**, 013626 (2018).
- [40] H. Tajima and S. Uchino, Thermal crossover, transition, and coexistence in Fermi polaronic spectroscopies, *Phys. Rev. A* **99**, 063606 (2019).
- [41] B. C. Mulkerin, X.-J. Liu, and H. Hu, Breakdown of the Fermi polaron description near Fermi degeneracy at unitarity, *Ann. Phys. (NY)* **407**, 29 (2019).
- [42] W. E. Liu, J. Levisen, and M. M. Parish, Variational approach for impurity dynamics at finite temperature,

- Phys. Rev. Lett. **122**, 205301 (2019).
- [43] J. Wang, X.-J. Liu, and H. Hu, Roton-induced Bose polaron in the Presence of synthetic spin-orbit coupling, Phys. Rev. Lett. **123**, 213401 (2019).
- [44] M. M. Parish, H. S. Adlong, W. E. Liu, and J. Levinsen, Thermodynamic signatures of the polaron-molecule transition in a Fermi gas, Phys. Rev. A **103**, 023312 (2021).
- [45] F. Isaule, I. Morera, P. Massignan, and Juliá-Díaz, Renormalization-group study of Bose polarons, Phys. Rev. A. **104**, 023317 (2021).
- [46] N. Syassen, D. M. Bauer, M. Lettner, T. Volz, D. Dietze, J. J. Garcia-Ripoll, J. I. Cirac, G. Rempe, and S. Dürr, Strong dissipation inhibits losses and induces correlations in cold molecular gases, Science **320**, 1329 (2008).
- [47] T. Tomita, S. Nakajima, I. Danshita, Y. Takasu, Y. Takahashi, Observation of the Mott insulator to superfluid crossover of a driven-dissipative Bose-Hubbard system, Sci. Adv., **3**, e1701513 (2017).
- [48] R. I. Bouganne, M. B. Aguilera, A. Ghermaoui, J. Beugnon and F. Gerbier, Anomalous decay of coherence in a dissipative many-body system, Nat. Phys. **16**, 21 (2020).
- [49] S. Lapp, J. Angógná, F. A. An and B. Gadway, Engineering tunable local loss in a synthetic lattice of momentum states, New J. Phys. **21** 045006 (2019).
- [50] J. Li, A. K. Harter, J. Liu, L. de Melo, Y. N. Joglekar, L. Luo, Observation of parity-time symmetry breaking transitions in a dissipative Floquet system of ultracold atoms, Nat. Commun, **10**, 855 (2019).
- [51] Y. Ashida, Z. Gong, and M. Ueda, Non-Hermitian Physics, Adv. Phys. **69**, 3 (2020).
- [52] J. Zhou, and W. Zhang, Fermi polaron in dissipative bath with spin-orbit coupling, EPL **134**, 30004 (2021).
- [53] J. Sun, Impurity in a Fermi gas under non-Hermitian spin-orbit coupling, Eur. Phys. J. D **75**, 39 (2021).
- [54] T. Wasak, R. Schmidt, and F. Piazza, Quantum-Zero Fermi-Polaron in the strong dissipation limit, Phys. Rev. Research **3**, 013086 (2021).
- [55] R. Combescot, A. Recati, C. Lobo and F. Chevy, Normal State of Highly Polarized Fermi Gases: Simple Many-Body Approaches, Phys. Rev. Lett. **98**, 180402 (2007).
- [56] W. E. Liu, J. Levinsen, M. M. Parish, Variational approach for impurity dynamics at finite temperature, Phys. Rev. Lett. **122**, 205301 (2019).
- [57] H. S. Adlong, W. E. Liu, F. Scazza, M. Zaccanti, N. D. Oppong, S. Fölling, M. M. Parish, and J. Levinsen, Quasiparticle lifetime of the repulsive Fermi polaron, Phys. Rev. Lett. **125**, 133401 (2020).
- [58] A. Kamenev, Field theory of non-equilibrium systems, 1st ed. (Cambridge University Press, 2011).
- [59] K. Yamamoto, M. Nakagawa, K. Adachi, K. Takasan, M. Ueda and N. Kawakami, Theory of Non-Hermitian Fermionic Superfluidity with a Complex-Valued Interaction, Phys. Rev. Lett. **123**, 123601 (2019).
- [60] H. Hu and X.-J. Liu, Fermi polarons at finite temperature: Spectral function and rf-spectroscopy, arXiv:2201.07872 (2022).
- [61] H. Deng, G. Weihs, C. Santori, J. Bloch, and Y. Yamamoto, Condensation of Semiconductor Microcavity Exciton Polaritons, Science **298**, 199 (2002).
- [62] J. Kasprzak, M. Richard, S. Kundermann, A. Baas, P. Jeambrun, J. M. J. Keeling, F. M. Marchetti, M. H. Szymańska, R. André, J. L. Staehli, V. Savona, P. B. Littlewood, B. Deveaud and L. S. Dang, Bose-Einstein condensation of exciton polaritons, Nature (London) **443**, 409 (2006).
- [63] R. Balili, V. Hartwell, D. Snoke, L. Pfeiffer and K. West, Bose-Einstein Condensation of Microcavity Polaritons in a Trap, Science **316**, 1007 (2007).
- [64] L. M. Sieberer, M. Buchhold and S. Diehl, Keldysh field theory for driven open quantum systems, Rep. Prog. Phys. **79** 096001 (2016).